

On the stability relations of hydrous minerals in water-undersaturated magmas

MARK S. GHIORSO

Department of Geological Sciences, Box 351310, University of Washington, Seattle, Washington 98195-1310, U.S.A.

ABSTRACT

Reaction of a hydrous mineral with a water-bearing silicate melt is analyzed in terms of the stoichiometry of (in)congruent dissolution. Application of the law of mass action provides an explanation for the presence of an isobaric thermal maximum that manifests itself in terms of enhanced stability of the phase under conditions of water undersaturation. It is shown that the water content of the melt at which the maximum develops is independent of pressure and water speciation, but is strongly dependent on the identity of other (“anhydrous”) melt species and upon the stoichiometric numbers of additional solid phases involved in the reaction. Utilizing MELTS, the analysis is applied to the cummingtonite-bearing rhyolitic magmas of the Taupo volcanic zone of New Zealand.

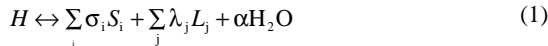
INTRODUCTION

Yoder and Kushiro (1969) first observed that in the isobaric incongruent melting of hydrous phlogopite, the temperature stability limit reaches a maximum under conditions where the resulting liquid is *undersaturated* with respect to a volatile phase of pure H₂O. Similar experimental observations on the melting of zoisite (Boettcher 1970) and pargasite (Holloway 1973), as well as related experimental work on amphibole stability in water-undersaturated Paricutin andesite (Eggler 1972), led Eggler (1973) to utilize Schreinemaker’s rules (e.g., Zen 1966) to develop an explanation for these stability relations. The Schreinemaker’s approach was later extended by Eggler and Holloway (1977) to include qualitative prediction in systems involving more than two thermodynamic components.

In this paper, an alternative thermodynamically based analysis of the conditions for a temperature maximum in the melting of hydrous phases in water-undersaturated magma is developed. This analysis is readily extendible to systems of arbitrary numbers of thermodynamic components, and can lead to quantitative predictions, if suitable activity-composition models are available for the phases involved.

THERMODYNAMIC ANALYSIS

Consider a hypothetical chemical reaction that embodies the crystallization or melting of a hydrous phase in a water-bearing magmatic system:



where H denotes a hydrous phase, reacting to form other solid phases (with components S_i) and a liquid, described in terms of components L_j , and H₂O. In Equation 1, the σ_i , λ_j , and α are stoichiometric reaction coefficients. Whereas H is assumed to

contain H₂O in the formula unit, that restriction does not necessarily apply to the S_i . The law of mass action relates an equilibrium constant (K) to the activities of thermodynamic components in the phases involved in a reaction. For the reaction in Equation 1:

$$K = \prod_i a_{S_i}^{\sigma_i} \prod_j a_{L_j}^{\lambda_j} a_{H_2O}^{\alpha} / a_H \quad (2)$$

where Π denotes a product of terms and a_i^j denotes the activity of the i^{th} component raised to the j^{th} power. Equation 2 may be expanded for further analysis by writing the activities of liquid components in terms of the products of activity coefficients (γ) and mole fractions (X):

$$K = \left(\prod_i a_{S_i}^{\sigma_i} \prod_j \gamma_{L_j}^{\lambda_j} \gamma_{H_2O}^{\alpha} / a_H \right) \prod_k X_{L_k}^{\lambda_k} (1 - X_{H_2O})^{\delta \lambda_k} X_{H_2O}^{(1+\delta)\alpha} \quad (3)$$

In Equation 3, the coefficient δ ($0 \leq \delta \leq 1$) is included to allow for the speciation of water in the melt in terms of molecular H₂O ($a_{H_2O} \propto X_{H_2O}$; $\delta = 0$) and hydroxyl species ($a_{H_2O} \propto X_{H_2O}^2$; $\delta = 1$). The term $(1 - X_{H_2O})^{\delta}$, which modifies the X_{L_k} , is required to satisfy Gibbs-Duhem relationships when δ is non-zero (see Appendix 3 of Ghiorso et al. 1983). To proceed with analysis of Equation 3, it will be assumed that the liquid components, L_k , have anhydrous compositions; i.e., H₂O is not a constituent in the formulas of these components. Consequently, the X_{L_k} may be written:

$$X_{L_k} = Y_{L_k} (1 - X_{H_2O}) \quad (4)$$

where the Y_{L_k} may be regarded as projected mole fractions of the liquid components on an anhydrous basis. With the definition of Equation 4, Equation 3 transforms to:

$$K = \left(\prod_i a_{S_i}^{\sigma_i} \prod_j \gamma_{L_j}^{\lambda_j} \prod_k Y_{L_k}^{\lambda_k} \gamma_{H_2O}^{\alpha} / a_H \right) (1 - X_{H_2O})^{(1+\delta)\sum_k \lambda_k} X_{H_2O}^{(1+\delta)\alpha} \quad (5)$$

The first parenthetical term on the right-hand side of Equation 5 is a function of X_{H_2O} only through the activity coefficients of liquid components. Therefore to first order, it is reasonable to assume that most of the variation in K with water content should

*E-mail: ghiorso@u.washington.edu

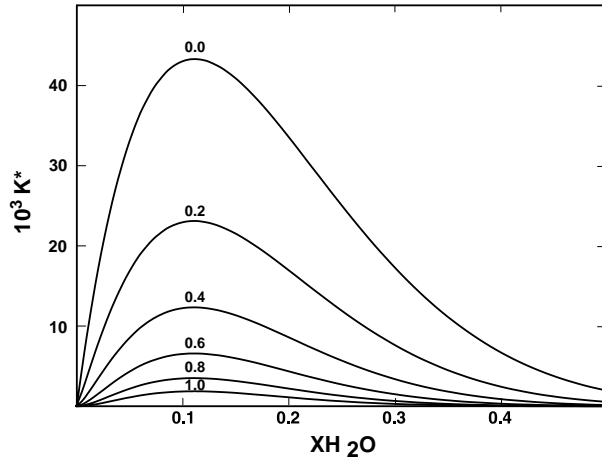


FIGURE 2. Variation of a modified equilibrium constant (K^*) for the reaction of cummingtonite with silicate melt plotted as a function of the mole fraction of water ($X_{\text{H}_2\text{O}}$) in the liquid. Reaction stoichiometry is given by Equation 7 and K^* is defined as $K^* = \frac{\kappa_{\Gamma}}{(1 - X_{\text{H}_2\text{O}})^{\delta(1+\delta)}(X_{\text{H}_2\text{O}})^{1+\delta}}$. Isoleths of K^* are labeled by δ .

consistent set of melt species appropriate to the temperature-pressure conditions of the experiment. To illustrate, Figure 2 is a plot of K^* vs. $X_{\text{H}_2\text{O}}$ for reaction 7 for six cases involving different assumptions regarding the speciation of water in the melt. The case of $a_{\text{H}_2\text{O}} \propto (X_{\text{H}_2\text{O}})^2$ ($\delta = 1$) is reproduced for reference (e.g., Fig. 1), and the case of $a_{\text{H}_2\text{O}} \propto X_{\text{H}_2\text{O}}$ ($\delta = 0$) represents the other extreme of water dissolved entirely as a molecular species. Intermediate cases are plotted corresponding to δ of 0.2, 0.4, 0.6, and 0.8. Note that $(X_{\text{H}_2\text{O}}^{\text{Tmax}})$ does not shift with δ (e.g., Eq. 9), but that the value of K^* at this maximum increases significantly (a factor of 20), with variation in δ . This pronounced increase in K^* translates into the magnitude of the thermal maximum that, consequently, is considerably more pronounced when water behaves predominantly as a molecular species in the melt. The case of varying $\sum_k \lambda_k$ is explored in Figure 3. Variation in $\sum_k \lambda_k$ results in an even more-pronounced effect on K^* and moves the thermal maximum to higher water contents. In practice, both variation in δ and $\sum_k \lambda_k$ may occur simultaneously, and of course the weak dependence of Γ on $X_{\text{H}_2\text{O}}^{\text{Tmax}}$ will affect the position and extent of the thermal maximum, but the potential exists to use experimental results of this kind to constrain and possibly distinguish alternate hypotheses of melt speciation. In this respect, the analysis of isobaric thermal maxima is analogous to the perhaps more familiar analysis of the variation of mineral solubility with pH, which yields insight into the stoichiometry of congruent dissolution of mineral phases into coexisting aqueous solution.

$X_{\text{H}_2\text{O}}^{\text{Tmax}}$ expressed as wt% H_2O dissolved in the melt

Given the potential for utilizing the position of the isobaric thermal maximum to document melt speciation, there is some motivation to recast the analysis in terms of experimentally determined quantities such as wt% dissolved H_2O rather than

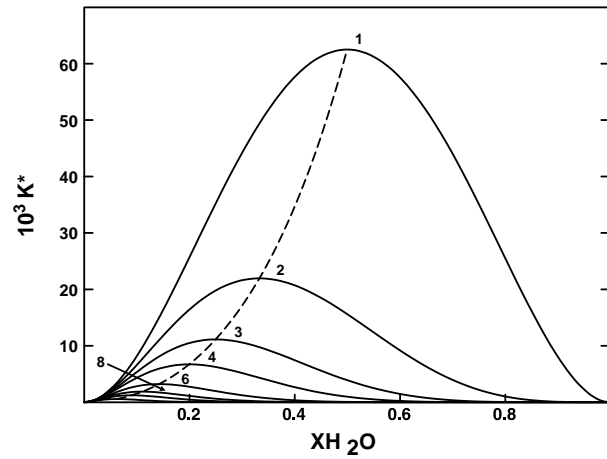


FIGURE 3. Variation of a modified equilibrium constant (K^*) for the reaction of cummingtonite with silicate melt plotted as a function of the mole fraction of water ($X_{\text{H}_2\text{O}}$) in the liquid. K^* is defined as $K^* = \frac{\kappa_{\Gamma}}{(1 - X_{\text{H}_2\text{O}})^{2\sum_k \lambda_k}} (X_{\text{H}_2\text{O}})^2$, and curves are plotted for variable reaction stoichiometry (e.g., Eqs. 7, 10, and 11), with $\sum_k \lambda_k$ equal to 1, 2, 3, 4, 6, 8, 10, 15. The dashed line defines the locus of thermal maximum for the range: $1 \leq \sum_k \lambda_k \leq 15$.

the model dependent $X_{\text{H}_2\text{O}}$. Defining K^* from Equation 6 as K/Γ , and taking w to denote the wt% H_2O dissolved in the melt, differentiation yields:

$$\frac{\partial K^*}{\partial w} = X_{\text{H}_2\text{O}}^{\delta} (1 - X_{\text{H}_2\text{O}})^{(1+\delta)\sum_k \lambda_k - 1} \left[2 - 2 \left(1 + \sum_k \lambda_k \right) X_{\text{H}_2\text{O}} \right] \frac{\partial X_{\text{H}_2\text{O}}}{\partial w}. \quad (12)$$

As the derivative, $\partial X_{\text{H}_2\text{O}}/\partial w$, must be positive ($X_{\text{H}_2\text{O}}$ is a monotonic function of w), zeroes in Equation 12 corresponding to extrema in K^* are given by $X_{\text{H}_2\text{O}}$ equal 0, 1, and $1/(1 + \sum_k \lambda_k / \alpha)$ (e.g., Eq. 9). Translation of the position of the thermal maximum from mole fraction to wt% H_2O is consequently straightforward and only involves expressing $X_{\text{H}_2\text{O}}^{\text{Tmax}}$ as a function of w . $X_{\text{H}_2\text{O}}$ may be written:

$$X_{\text{H}_2\text{O}} = \frac{\frac{w}{MW_w}}{\frac{w}{MW_w} + \sum_i \frac{c_i}{MW_i}} \quad (13)$$

where MW_i denotes the molecular weight of the i^{th} melt component and c_i refers to the concentration, in weight percent, of melt components other than water. The c_i in Equation 13 may be recast in terms of component concentrations in an equivalent anhydrous melt ($c_i^{\text{anhy}} = c_i / [100 - w]$):

$$X_{\text{H}_2\text{O}} = \frac{\frac{w}{MW_w}}{\frac{w}{MW_w} + \frac{100 - w}{100} \sum_i \frac{c_i^{\text{anhy}}}{MW_i}} \quad (14)$$

Equating Equations 9 and 14,

$$X_{\text{H}_2\text{O}}^{\text{max}} = \frac{1}{1 + \frac{\sum_k \lambda_k}{\alpha}} = \frac{1}{1 + \frac{MW_w(100 - w^{\text{max}})}{100w^{\text{max}}} \sum_i \frac{c_i^{\text{anhy}}}{MW_i}} \quad (15)$$

gives the relation

$$\frac{\sum_k \lambda_k}{\alpha} = \frac{MW_w(100 - w^{\text{max}})}{100w^{\text{max}}} \sum_i \frac{c_i^{\text{anhy}}}{MW_i} \quad (16)$$

from which the position of the thermal maximum, in terms of wt% H₂O (w^{max}), is given by:

$$w^{\text{max}} = \frac{MW_w}{\frac{MW_w}{100} + \frac{\sum_k \lambda_k}{\alpha \sum_i \frac{c_i^{\text{anhy}}}{MW_i}}} \quad (17)$$

For further analysis, it is convenient to introduce the linear transformation, $\lambda_k = \sum_j M_{kj} \lambda_j^{\text{ox}}$, which maps stoichiometric coefficients for oxide components, λ_j^{ox} , to those of the component set chosen. This same linear transformation relates, *in part*, moles of oxides to moles of melt components. It is an incomplete mapping however, because all melt components may not be involved in the reaction of the hydrous mineral with the melt (e.g., the mineral-melt reaction may be given by Eq. 7 and K₂O may be present in the melt). Therefore, the more general linear transformation

$$\frac{c_i^{\text{anhy}}}{MW_i} = \sum_j M_{ij} \frac{c_j^{\text{anhy,ox}}}{MW_j} + \sum_j N_{ij} \frac{c_j^{\text{anhy,ox}}}{MW_j} \quad (18)$$

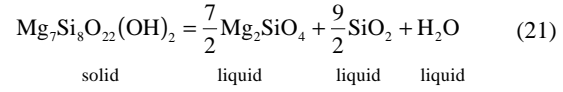
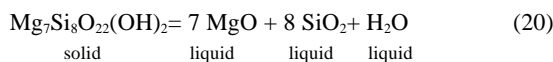
is adopted, where the second term accounts for those melt components not participating in the mineral-melt reaction. These definitions allow Equation 17 to be written as:

$$w^{\text{max}} = \frac{MW_w}{\frac{MW_w}{100} + \frac{\sum_k \sum_j M_{kj} \lambda_j^{\text{ox}}}{\alpha \sum_i \left(\sum_j M_{ij} \frac{c_j^{\text{anhy,ox}}}{MW_j^{\text{ox}}} + \sum_j N_{ij} \frac{c_j^{\text{anhy,ox}}}{MW_j^{\text{ox}}} \right)}} \quad (19)$$

This expression is the “wt% equivalent” of Equation 9.

It is apparent from inspection of Equation 19 that altering the concentration of any oxide in the melt ($c_j^{\text{anhy,ox}}$) will move the position of the thermal maximum (w^{max}). This result is intuitive and consistent with experimental observations (e.g., Yoder and Kushiro 1969). The effect of changing melt speciation however, is more subtle. Two simple examples will illustrate.

Consider the pair of equations:



illustrating the reaction of end-member magnesio-cummingtonite and silicate melt with two different choices of melt speciation. If the melt composition lies in the system MgO-SiO₂-H₂O, then Equation 19 may be written:

$$w^{\text{max}} = \frac{MW_w}{\frac{MW_w}{100} + \frac{(M_{1,\text{SiO}_2} + M_{2,\text{SiO}_2})8 + (M_{1,\text{MgO}} + M_{2,\text{MgO}})7}{\alpha \left[(M_{1,\text{SiO}_2} + M_{2,\text{SiO}_2}) \frac{c_{\text{SiO}_2}^{\text{anhy,ox}}}{MW_{\text{SiO}_2}^{\text{ox}}} + (M_{1,\text{MgO}} + M_{2,\text{MgO}}) \frac{c_{\text{MgO}}^{\text{anhy,ox}}}{MW_{\text{MgO}}^{\text{ox}}} \right]}} \quad (22)$$

Assuming “oxide” melt species are chosen (e.g., Eq. 20), Equation 22 reduces to

$$w^{\text{max}} = \frac{MW_w}{\frac{MW_w}{100} + \frac{15}{\alpha \left[\frac{c_{\text{SiO}_2}^{\text{anhy,ox}}}{MW_{\text{SiO}_2}^{\text{ox}}} + \frac{c_{\text{MgO}}^{\text{anhy,ox}}}{MW_{\text{MgO}}^{\text{ox}}} \right]}} \quad (23)$$

Alternatively, if melt species corresponding to the reaction in Equation 21 are chosen, then M is given by

$$\begin{bmatrix} M_{\text{Mg}_2\text{SiO}_4,\text{MgO}} & M_{\text{SiO}_2,\text{MgO}} \\ M_{\text{Mg}_2\text{SiO}_4,\text{SiO}_2} & M_{\text{SiO}_2,\text{SiO}_2} \end{bmatrix} = \begin{bmatrix} \frac{1}{2} & 0 \\ -\frac{1}{2} & 1 \end{bmatrix}$$

and Equation 22 reduces to:

$$w^{\text{max}} = \frac{MW_w}{\frac{MW_w}{100} + \frac{(-\frac{1}{2} + 1)8 + (\frac{1}{2} + 0)7}{\alpha \left[(-\frac{1}{2} + 1) \frac{c_{\text{SiO}_2}^{\text{anhy,ox}}}{MW_{\text{SiO}_2}^{\text{ox}}} + (\frac{1}{2} + 0) \frac{c_{\text{MgO}}^{\text{anhy,ox}}}{MW_{\text{MgO}}^{\text{ox}}} \right]}} \quad (24)$$

Equation 24 is *identical* to Equation 23; the position of the thermal maximum, expressed in terms of wt% H₂O, is not displaced by changing $\sum_k \lambda_k$ from 15 (Eq. 20) to 8 (Eq. 21), unlike $X_{\text{H}_2\text{O}}^T$ (Fig. 3). It can be shown that any choice of melt speciation model that can be expressed in terms of a linear transformation of oxides yields a similar conclusion. The w^{max} related to melting of magnesio-cummingtonite in the system MgO-SiO₂-H₂O is insensitive to melt speciation. Interestingly, this is not the whole story in an extended chemical system. Consider a second example of the reaction of magnesio-cummingtonite according to Equations 20 and 21 with a melt composition in the system MgO-Al₂O₃-SiO₂-H₂O. Equation 19 now becomes

$$w^{\text{max}} = \frac{MW_w}{\frac{MW_w}{100} + \frac{15}{\alpha \left[\frac{c_{\text{SiO}_2}^{\text{anhy,ox}}}{MW_{\text{SiO}_2}^{\text{ox}}} + \frac{c_{\text{MgO}}^{\text{anhy,ox}}}{MW_{\text{MgO}}^{\text{ox}}} + \frac{c_{\text{Al}_2\text{O}_3}^{\text{anhy,ox}}}{MW_{\text{Al}_2\text{O}_3}^{\text{ox}}} \right]}} \quad (25)$$

for the case of Equation 20 and

$$w^{\max} = \frac{MW_w}{100} + \frac{MW_w}{15} \alpha \left[\frac{C_{\text{SiO}_2}^{\text{anhy,ox}}}{MW_{\text{SiO}_2}^{\text{ox}}} + \frac{C_{\text{MgO}}^{\text{anhy,ox}}}{MW_{\text{MgO}}^{\text{ox}}} + 2 \frac{C_{\text{Al}_2\text{O}_3}^{\text{anhy,ox}}}{MW_{\text{Al}_2\text{O}_3}^{\text{ox}}} \right] \quad (26)$$

for the case of Equation 21, including the simplifying assumption that Al_2O_3 is the sole Al-bearing melt species. It is apparent that Equations 25 and 26 are not identical and, consequently, it follows that w^{\max} shifts with melt speciation in the system containing alumina. This example generalizes to the conclusion that melt speciation will affect the value of w^{\max} if the reaction involving mineral and melt is examined in a supersystem of the composition-space of the mineral. Thus, for minerals crystallizing from magmatic composition melts, the dependence of w^{\max} on melt speciation is to be expected.

Effect of incongruent melting on $X_{\text{H}_2\text{O}}^T$

The results displayed in Figure 3 also demonstrate the effect of incongruent dissolution/precipitation (non-zero σ_i in Eq. 1). Additional solid phases (S_i) involved in the reaction of H with melt will modify the stoichiometric coefficients λ_i and possibly α , thereby shifting the position and extent of the thermal maximum. In the typical case of incongruent reaction involving the production of “anhydrous” solid phases, the shift in $X_{\text{H}_2\text{O}}^T$ will be toward higher water contents and more pronounced temperature extrema (i.e., smaller $\sum_k \lambda_k$, Fig. 3).

AN EXAMPLE UTILIZING MELTS

A quantitative example of the significance of the water-undersaturated thermal maximum with respect to the stability of cummingtonite in rhyolitic magmas can be constructed with the aid of the MELTS software package (Ghiorso and Sack 1995). For this example, a magma bulk composition corresponding to an average cummingtonite-bearing rhyolite lava from the Taupo volcanic region of New Zealand (Table 11-6, no. 5, p. 554 of Carmichael et al. 1974) was chosen for analysis. Estimation of the thermal maximum for cummingtonite saturation is made by calculating with MELTS the liquidus temperature for that phase at specified water content and total pressure. All other solid phases are suppressed from forming so that liquid-cummingtonite stability relations for this bulk composition can be analyzed unambiguously. Results for five isobars are displayed in Figure 4. Also shown is the water saturation limit for a magma of this bulk composition as modeled by MELTS.

There is a striking similarity between the isobars shown in Figure 4 and the $K^*-X_{\text{H}_2\text{O}}$ curve drawn in Figure 1, both in terms of overall shape and in the position of the thermal maximum at $X_{\text{H}_2\text{O}} \approx 0.11$. This is due in large part to the fact that in MELTS, the chemical reaction for cummingtonite saturation is given by Equation 7, with $a_{\text{H}_2\text{O}} \propto X_{\text{H}_2\text{O}}^2$. The similarity also confirms the assumption made above that compositional variation in activity coefficients for melt components contribute only second-order effects with respect to the major features of the thermal maximum. The most notable aspect of the results displayed in

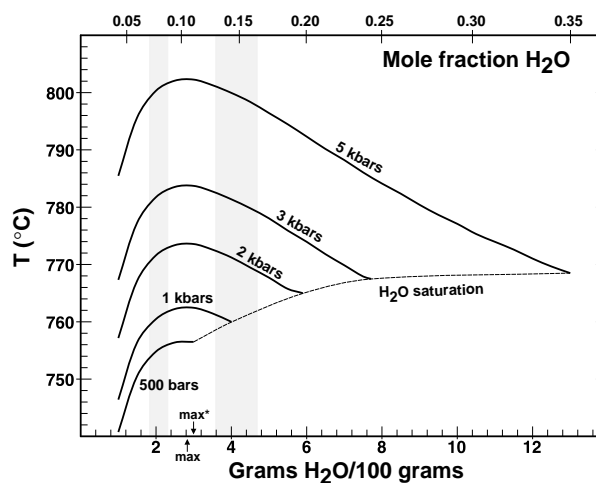


FIGURE 4. Liquidus temperature for Mg,Fe-cummingtonite in bulk compositions corresponding to rhyolites from the Taupo volcanic region of New Zealand (see text), calculated as a function of water content using MELTS (Ghiorso and Sack 1995). The calculated water saturation curve from MELTS is also plotted for reference. Vertical bars correspond to water contents of typical amphiboles (centered around 2) and micas (centered around 4). max^* points to the theoretical maximum calculated from Equation 9 and max points to the maximum calculated by MELTS; the difference between the two demonstrates the dependence of melt component activity coefficients on H_2O content.

Figure 4 is that $X_{\text{H}_2\text{O}}^T$ is essentially independent of pressure. This result could have been anticipated, as it follows from the experimental observation that the partial molar volume of dissolved H_2O is independent of melt composition (Lange 1994). However, because of this invariance and the strong effect of pressure on $X_{\text{H}_2\text{O}}^{\text{sat}}$, the thermal maximum will appear at higher degrees of water-undersaturation as pressure on the system is increased, and the magnitude of the thermal maximum will be more significant the higher the pressure.

It should be noted that the calculated thermal maximum in Figure 4 could be shifted to higher water contents (and probably higher temperatures) if the precipitation of cummingtonite from the magma involves a reaction with some other solid phase. This shift can be accomplished by altering the reaction stoichiometry to correspond to smaller values of $\sum_k \lambda_k$ (e.g., Fig. 3). Justification for this interpretation follows from the petrographic observation that hornblende and cummingtonite are rarely found together in the phenocryst assemblages of the Taupo lavas (Ewart et al. 1971), whereas other phases are equally likely to be found with either amphibole. The formation of cummingtonite in this magmatic system probably involves a reaction of hornblende with melt, which may be represented in the form of Equation 1 with non-zero σ for the cummingtonite component in hornblende and with consequently smaller $\sum_k \lambda_k$. This line of reasoning may provide an explanation for the stability of cummingtonite at elevated pressures and temperatures in magmatic systems that are close to water saturation. In the absence of some form of incongruent reaction between cummingtonite, melt, and some additional solid phase,

cumingtonite will breakdown as temperature and/or water content of the melt is increased. Persistence of cumingtonite under these conditions implies a shift in the thermal maximum that is more likely driven by reaction stoichiometry changes induced by incongruency rather than dramatic changes in melt speciation.

ACKNOWLEDGMENTS

As usual, after having accidentally stumbled upon the effect analyzed in this paper by experimenting with MELTS, Bernard Evans introduced me to the literature on this subject. I am grateful as well to Victor Kress, who offered his usual enthusiasm and thoughtful criticism. Helpful reviews by Bernard Evans, Tim Grove, Michel Pichavant, and Victor Kress resulted in improvements to the manuscript and the incorporation of an analysis of the movement of the thermal maximum as a function of wt% H₂O. Material support was provided by the National Science Foundation (OCE-9529790).

REFERENCES CITED

- Boettcher, A.L. (1970) The system CaO-Al₂O₃-H₂O at high pressures and temperatures. *Journal of Petrology*, 11, 337-379.
- Burnham, C.W. (1994) Development of the Burnham model for prediction of H₂O solubility in magmas. In *Mineralogical Society of America Reviews in Mineralogy*, 30, 123-129.
- Carmichael, I.S.E., Turner, F.J., and Verhoogen, J. (1974) *Igneous Petrology*. McGraw-Hill, New York, 739 p.
- Eggler, D.H. (1972) Amphibole stability in H₂O-undersaturated calc-alkaline melts. *Earth and Planetary Science Letters*, 15, 28-34.
- (1973) Principles of melting of hydrous phases in silicate melt. *Carnegie Institution of Washington, Yearbook* 72, 491-495.
- Eggler, D.H. and Holloway, J.R. (1977) Partial melting of peridotite in the presence of H₂O and CO₂: Principles and review. In H.J.B. Dick, Ed., *Magma Genesis. Bulletin, State of Oregon, Department of Geology and Mineral Resources*, 96, 15-36.
- Ewart, A., Green, D.C., Carmichael, I.S.E., and Brown, F.H. (1971) Voluminous low temperature rhyolitic magmas in New Zealand. *Contributions to Mineralogy and Petrology*, 33, 128-144.
- Ghiorso, M.S. and Sack, R.O. (1995) Chemical mass transfer in magmatic processes IV. A revised and internally consistent thermodynamic model for the interpolation and extrapolation of liquid-solid equilibria in magmatic systems at elevated temperatures and pressures. *Contributions to Mineralogy and Petrology*, 119, 197-212.
- Ghiorso, M.S., Carmichael, I.S.E., Rivers, M.L., and Sack, R.O. (1983) The Gibbs free energy of mixing of natural silicate liquids; an expanded regular solution approximation for the calculation of magmatic intensive variables. *Contributions to Mineralogy and Petrology*, 84, 107-145.
- Holloway, J.R. (1973) The system pargasite-H₂O-CO₂: a model for melting of a hydrous mineral with a mixed-volatile fluid - I. Experimental results to 8 kbar. *Geochimica et Cosmochimica Acta*, 37, 651-666.
- Lange, R.A., (1994) Densities and viscosities of water-bearing silicate liquids. In *Mineralogical Society of America Reviews in Mineralogy*, 30, 123-129.
- Yoder Jr., H.S., and Kushiro, I. (1969) Melting of a hydrous phase: Phlogopite. *American Journal of Science*, 267-A, 558-582.
- Zen, E-an (1966) Construction of pressure-temperature diagrams for multicomponent systems after the method of Schreinemakers —A geometric approach. *Bulletin of the United States Geological Survey*, 1225, 56 p.

MANUSCRIPT RECEIVED DECEMBER 12, 1997

MANUSCRIPT ACCEPTED MAY 24, 1999

PAPER HANDLED BY ROBERT W. LUTH